Multifractal scaling analyses of the spatial diffusion pattern

of COVID-19 pandemic in Chinese mainland

Yuqing Long, Yanguang Chen, Yajing Li

(Department of Geography, College of Urban and Environmental Sciences, Peking University,

Beijing 100871, P.R.China. E-mail: chenyg@pku.edu.cn)

Abstract: Revealing spatiotemporal evolution regularity in the spatial diffusion of epidemics is

helpful for preventing and controlling the spread of epidemics. Based on the real-time COVID-19

datasets by prefecture-level cities and date, this paper is aimed at exploring the multifractal scaling

in spatial diffusion pattern of COVID-19 pandemic and its evolution characteristics in Chinese

mainland. The ArcGIS technology and box-counting method are employed to extract spatial data

and the least square calculation is used to calculate fractal parameters. The results show multifractal

distribution of COVID-19 pandemic in China. The generalized correlation dimension spectrums are

inverse S-shaped curves, but the fractal dimension values significantly exceeds the Euclidean

dimension of embedding space when moment order q << 0. The local singularity spectrums are

asymmetric unimodal curves, which slant to right. The fractal dimension growth curves are shown

as quasi S-shaped curves. From these spectrums and growth curves, the main conclusions can be

drawn as follows. First, self-similar patterns developed in the process of Covid-19 pandemic, which

seem be dominated by multi-scaling law. Second, the spatial pattern of COVID-19 across China can

be characterized by global clustering with local disordered diffusion. Third, the spatial diffusion

process of COVID-19 in China experienced four stages, i.e., initial stage, the rapid diffusion stage,

the hierarchical diffusion stage, and finally the contraction stage. This study suggests that

multifractal theory can be utilized to characterize spatio-temporal diffusion of COVID-19 pandemic,

and the case analyses may be instructive for further exploring natural laws of spatial diffusion.

Keywords: COVID-19; spatial diffusion; spatial isolation; multifractals; fractal dimension growth

curve; Chinese mainland

1

1. Introduction

Human beings have long been suffered from various rapidly spread epidemics. It is significant to research the spatial diffusion regularity of infectious diseases. The most recent case of epidemic outbreak is the well-known coronavirus (COVID-19) in December 2019 (Huang et al., 2020; Mehta et al., 2020). Studies on the spatial diffusion pattern of COVID-19 are not only helpful for understanding its transmission dynamics, but also for the future prevention and control of epidemics. In literature, many studies have analyzed and modeled the spatio-temporal pattern of epidemics by various mathematical methods (Meng et al., 2005; Wang et al., 2008; Fang et al., 2009; Kang et al., 2020; Wu et al., 2020; YeşİLkanat, 2020; Zhao and Chen, 2020). Conventional mathematical methods are based on the mathematical concept of characteristic scale. If a spatial distribution bear no characteristic length, conventional mathematical modelling will be ineffective. In this case, the modeling idea from characteristic scale should be replaced by that from scaling. Fractal geometry provides a powerful tool for scaling analysis (Mandelbrot, 1982), and has been widely used to characterize complex systems (Batty and Longley, 1994; Frankhauser, 1998; Chen, 2014a; Chen and Huang, 2019). In this study, we propose a multifractal scaling model to capture the complex pattern and process of spatial epidemic dynamics.

Multifractal scaling analysis bears analogy with telescopes and microscopes in spatial analysis. It provides two sets of parameter spectrums adequately quantifying the spatial patterns and the statistical distribution of measurements across spatial scales (Stanley and Meakin, 1988; Pavon-Dominguez *et al.*, 2017). In recent years, growing studies have employed multifractal scaling modeling to geospatial pattern analysis (Chen and Wang, 2013; Murcio *et al.*, 2015; Salat *et al.*, 2018; Frankhauser *et al.*, 2018; Man *et al.*, 2019). Multifractal measures reflect a distribution of physical or other quantities on a geometric support (Feder, 1988). The spatial diffusion pattern of the epidemic is also the reflection of spatial organization patterns and cascade system of human social and economic activities (Wang *et al.*, 2020). Previous studies have found that the spatial distribution of population exhibits multifractal structure (Semecurbe *et al.*, 2016; Appleby, 1996; Chen and Shan, 1999; Liu and Liu, 1993). And the epidemic infections spread among the population. Population may be the geometric support of multifractal distribution of Covid-19 pandemic. In this study, we are trying to figure out whether the spatial diffusion pattern of COVID-19 shows

multifractal characteristics as well, and what can be learned from the spatio-temporal analysis of multifractal scaling model.

To address the above problems, we perform the multifractal scaling analyses to quantify the spatial diffusion pattern of COVID-19 pandemic and its evolution characteristics in Chinese mainland. First of all, we establish a spatial database of COVID-19 infections by prefecture-level cities and date. Then, the functional box-counting method and the ordinary least square regression method are employed to calculate the global and local multifractal parameters. The remainder of this paper is organized as follows. In Section 2, the multifractal scaling model and dataset used in this study are introduced. Section 3 details the main results of multifractal analyses. The multifractal characteristics of the spatial pattern of COVID-19 are examined, and then two sets of multifractal spectrums are employed to reveal detailed characteristics of the spatial diffusion pattern. Finally, the spatial diffusion process and its stage features are illustrated by the fractal dimension growth curves. In Section 4, the key points of the analyzed results are outlined, and related questions are discussed. Finally, Section 5 summarizes the main inferences of the spatial diffusion pattern of COVID-19 pandemic.

2. Methodology and materials

2.1 Multifractal model

A multifractal system is a self-similar hierarchy with cascade structure, which is based on two or more scaling processes (Chen, 2019) (Figure 1(a)). Multifractals are also known as multi-scaling fractals. Therefore, different subareas have different scaling behaviors and growth probabilities, i.e., the denser and sparser zones may display different spatial characteristics, leading to a heterogeneous distribution. Therefore, a single fractal dimension is difficult to fully explain the patterns and processes of complex systems in the real world (Chen, 2014; Murcio *et al.*, 2015). The multifractal analyses provide a series of parameters to capture detailed information about the rich structure at fine scales, which finally appear synthesized in a multifractal spectrum of parameters (Caniego *et al.*, 2005) (Figure 1(b)). Generally, two sets of parameters are employed in multifractal analyses, including global and local parameters. The global parameters include *generalized correlation dimension*, D(q), and *mass exponent*, $\tau(q)$, and the local parameters comprise *singularity exponent*,

 $\alpha(q)$, and local fractal dimension of the fractal subsets, f(q).

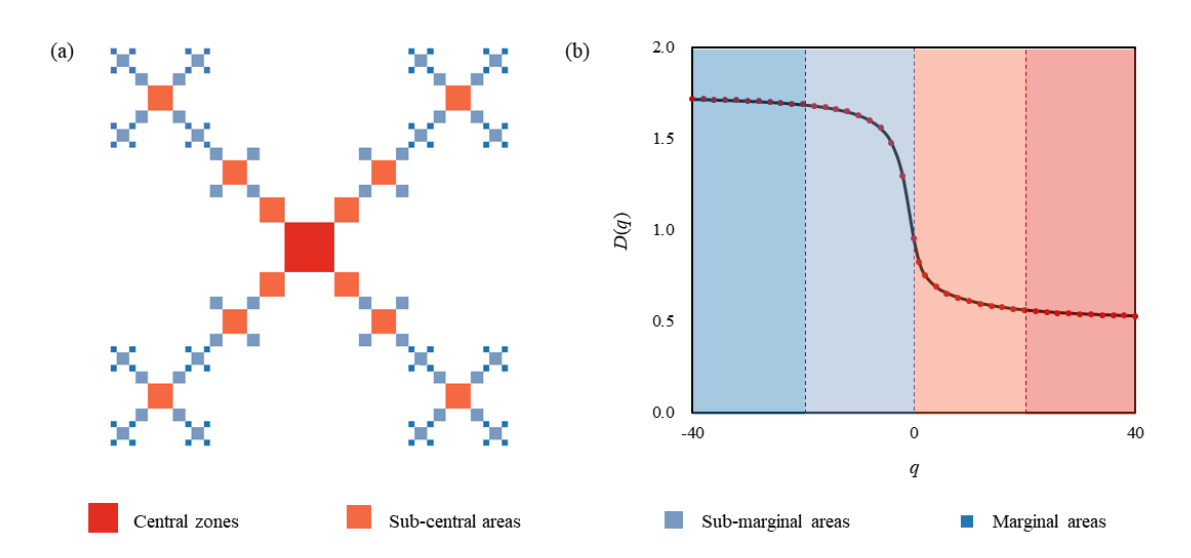


Figure 1. Schematic illustration of how different dominant structures of systems are projected to the multifractal spectrums. (a) Different hierarchical structures of regular multifractals. (b) The multifractal spectrums composed of a series of multifractal parameters

Global parameters describe the research object from the macro level. The generalized correlation dimension D(q) is based on Renyi's information entropy, expressed as (Hentschel and Procaccia, 1983; Feder, 1988; Vicsek, 1989):

$$D(q) = -\lim_{\varepsilon \to 0} \frac{I_{q}(\varepsilon)}{\ln \varepsilon} = \begin{cases} \frac{1}{q - 1} \lim_{\varepsilon \to 0} \frac{\ln \sum_{i=1}^{N(\varepsilon)} P_{i}(\varepsilon)^{q}}{\ln \varepsilon}, & (q \neq 1) \\ \frac{\sum_{i=1}^{N(\varepsilon)} P_{i}(\varepsilon) \ln P_{i}(\varepsilon)}{\ln \varepsilon}, & (q = 1) \end{cases}$$

$$(1)$$

where q refers to the moment order $(-\infty < q < \infty)$, $I_q(\varepsilon)$ to the Renyi's entropy with a linear scale ε . $N(\varepsilon)$ refers to the number of nonempty boxes, and $P_i(\varepsilon)$ represents the growth probability, indicating the ratio of measurement results of fractal subset appearing in the ith box $L_i(\varepsilon)$ to that of whole fractal copies $L(\varepsilon)$; that is, $P_i(\varepsilon) = L_i(\varepsilon) / L(\varepsilon)$. At a specific scale ε , the larger $P_i(\varepsilon)$ with higher growth probability corresponds to central regions. Therefore, by changing the value of q, attention can be focused on regions with high growth probability $(q \rightarrow \infty)$, or, conversely, on regions with low growth probability $(q \rightarrow \infty)$ (Figure 1). Another global parameter, mass exponent $\tau(q)$ can be estimated by

D(q) (Halsey et al., 1986; Feder, 1988):

$$\tau(q) = (q-1)D(q). \tag{2}$$

It reflects the properties from the viewpoint of mass. The global analysis is focused on the generalized correlation dimension D(q).

Local parameters focus on the micro-level in a multifractal system. Given to its heterogeneity, the multifractal system has many fractal subsets, and each part corresponds to a power law:

$$P_i(\varepsilon) \propto \varepsilon_i^{\alpha(q)},$$
 (3)

where ε_i refers to the corresponding linear scale of the *i*th box. And $\alpha(q)$ refers to the strength of local singularity, also known as *Lipschitz-Hölder singularity exponent*, suggesting the degree of singular interval measures (Feder, 1988). Different values of α correspond to different subsets of multifractals. Accordingly, the number of fractal subsets with the same α value under the linear ε_i is given by

$$N(\alpha, \varepsilon_i) \propto \varepsilon_i^{-f(\alpha)},$$
 (4)

where $f(\alpha)$ refers to the *local fractal dimension*. Therefore, the different subset will also have a corresponding fractal dimension, composing a singularity spectrum $f(\alpha)$ that changes along with $\alpha(q)$ to describe the corresponding changes in the subsystem (Song and Yu, 2019).

The multifractal dimension is defined based on entropy and correlation function. With the help of entropy, the spatial difference and space-filling pattern of COVID-19 can be characterized. With the help of correlation function, the diffusion mechanism and controlled degree of COVID-19 can be revealed. In this study, the main measure indexes are as follows: the generalized correlation dimension spectrum D(q), the local singularity spectrum $f(\alpha)$ and three representative fractal dimensions: the *capacity dimension* D_0 , the *information dimension* (*Shannon entropy*) D_1 , and the *correlation dimension* D_2 (Grassberger, 1983).

2.2 Data sources

The COVID-19 dataset by prefecture-level cities and date is obtained from the real-time authorized reports from the National Health Commission and the provincial health commissions. We collect the cumulative number of confirmed cases in Chinese mainland from Jan 11 to Feb 29, 2020, which was during the pandemic period of COVID-19 in China. Then, the COVID-19 dataset

is matched with the latest administrative units of prefecture-level cities in ArcGIS 10.2. The spatial analysis database of COVID-19 is established.

The multifractal parameters of the spatial pattern of COVID-19 can be calculated by functional box-counting method. First of all, determine a study area for fractal measurement. We make a box nearly covering the whole range of Chinese mainland as our study area (Figure 2). Second, transform each prefecture-level administrative unit into a point according to its geographic center. Third, iteratively divide the box into four equal boxes, and make intersections with the point dataset. Then, count the number of points in each box and the cumulative number of confirmed cases. Finally, estimate the multifractal parameters by the ordinary least squares regression method based on Eq(1)-(4) (Chen and Wang, 2013).

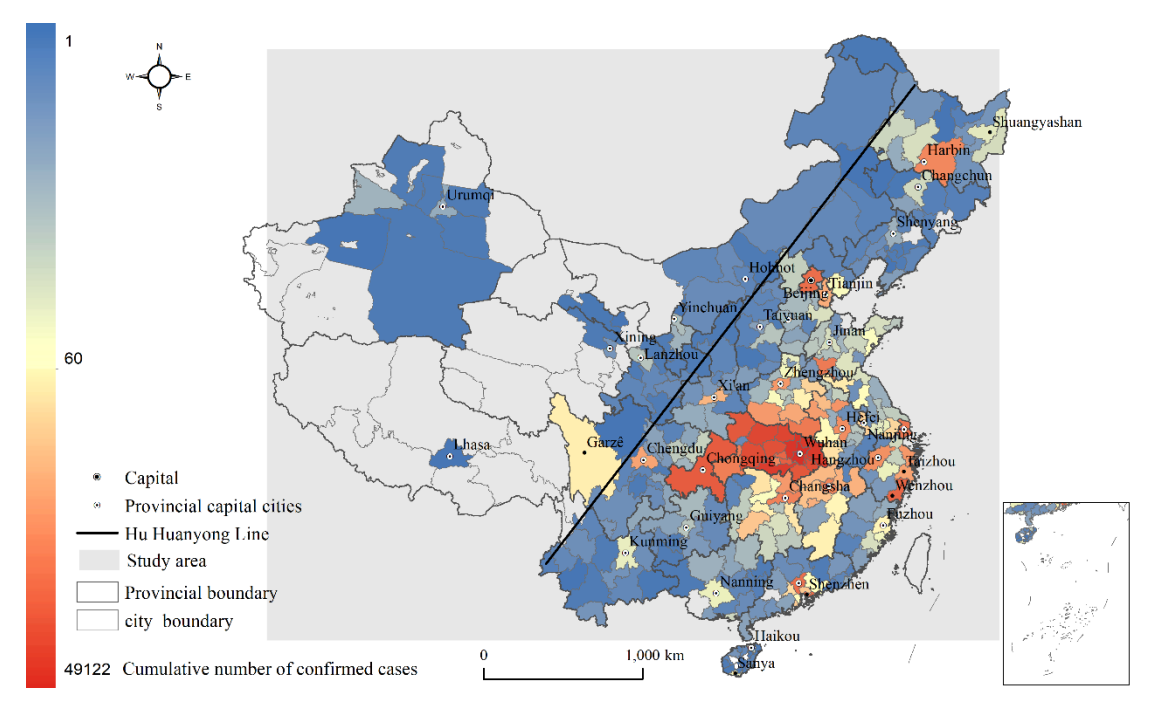


Figure 2. Spatial distribution of the cumulative confirmed cases of COVID-19 in Chinese mainland (up to Feb 29, 2020)

3. Results

3.1 Multifractal characteristics of the spatial pattern of COVID-19

The log-log plots reflect the fractal features of the spatial pattern of COVID-19, and then its multifractal characteristics are revealed by the global and local fractal dimension spectrums. First of all, the spatial pattern of COVID-19 displays fractal features, but its fractal structure is not well-

developed. As seen in Table 1, the model has significant double logarithmic linear relation, indicating there is an obvious fractal nature of the spatial pattern of COVID-19. And $D_0 > D_1 > D_2$ significantly. However, the log-log plots show that the fitness is not so satisfying when $q \neq 0$ (Figure 3), implying a poor-developed fractal structure. Then, the global and local multifractal parameters are calculated to obtain the corresponding generalized correlation dimension spectrum D(q), and the local singularity spectrum $f(\alpha)$ (Figure 4). The D(q) spectrums are inverse S-shaped curves, rather than horizontal lines. And the $f(\alpha)$ spectrums are winding unimodal curves, instead of a single point. Both of them display typical signs of multifractal features. These calculations provide further evidence that the spatial pattern of COVID-19 presents significant multifractal characteristics.

Table 1 Simple fractal dimensions of the spatial diffusion pattern of COVID-19 in Chinese mainland (partial results)

Date	Capacity dimension D_0	R^2	Information dimension D_1	R^2	Correlation dimension D_2	R ²
Jan	0.5369**	0.906	0.1033*	0.815	0.0423*	0.721
20	(0.0861)	8	(0.0246)	1	(0.0132)	1
Jan	1.4399***	0.991	0.9960***	0.991	0.5729***	0.990
25	(0.0656)	8	(0.0460)	5	(0.0288)	0
Jan	1.5321***	0.994	0.9964***	0.983	0.6052***	0.973
30	(0.0595)	0	(0.0649)	3	(0.0502)	2
	1.5589***	0.995	0.8561***	0.975	0.4671***	0.958
Feb 5	(0.0551)	0	(0.0682)	3	(0.0486)	4
Feb	1.5598***	0.995	0.7792***	0.972	0.397***	0.957
10	(0.0547)	1	(0.0654)	6	(0.0420)	2
Feb	1.5607***	0.995	0.6112***	0.967	0.2714***	0.956
15	(0.0544)	2	(0.0556)	9	(0.0291)	0
Feb	1.5607***	0.995	0.5852***	0.968	0.2538***	0.957
20	(0.0544)	2	(0.0532)	0	(0.0269)	1
Feb	1.5607***	0.995	0.5747***	0.967	0.2472***	0.956
25	(0.0544)	2	(0.0526)	6	(0.0262)	9
Feb	1.5607***	0.995	0.5658***	0.967	0.2414***	0.957
29	(0.0544)	2	(0.0516)	8	(0.0255)	4

Note: The robust Standard Errors are quoted in parenthesis. *** significant at 1%; ** significant at 5%; * significant at 10%.

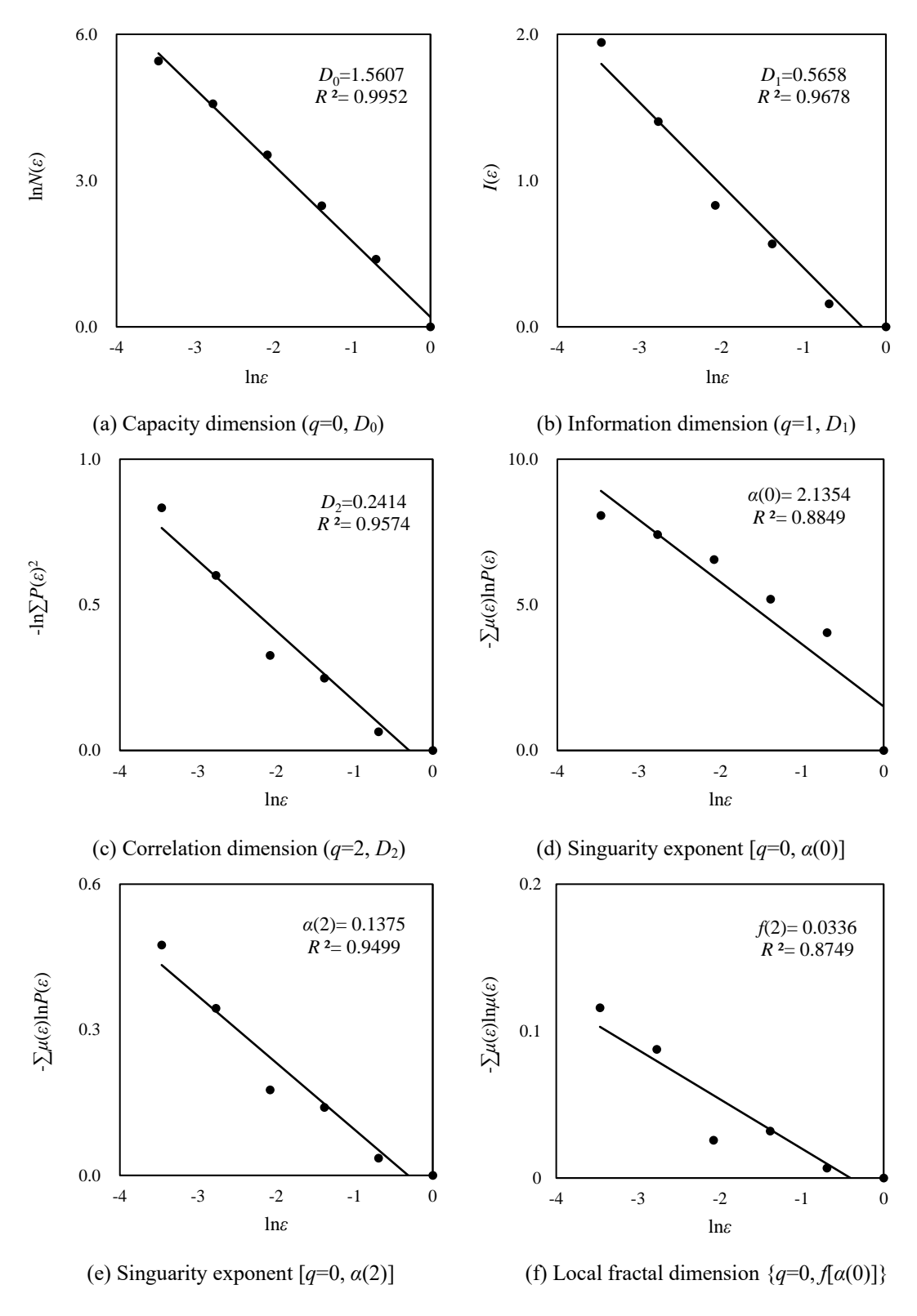


Figure 3. The log-log plots of estimating multifractal parameters of the spatial pattern of COVID-19 on Feb 29, 2020 (examples)

3.2 Multifractal spectrum analysis

The combination of global and local multifractal spectrums reflects the spatial diffusion characteristics of COVID-19. Firstly, we focus on the global multifractal spectrums, namely D(q) spectrum. Considering the spatial diffusion network of COVID-19 infections as a hierarchy, when $q \rightarrow +\infty$, the central regions with more infections would be brought into focus, especially in Wuhan and its surrounding areas, as well as some sub-central areas. Conversely, when $q \rightarrow -\infty$, the sparse regions with few infections will be highlighted, mainly in the edge areas or remote areas affected by COVID-19. In the D(q) spectrum (Figure 4(a)), the convergence value of D(q) decreased slowly when q>0. This suggests that the spatial diffusion of COVID-19 in central regions was strictly confined by the lockdown measures. However, when q<0, the convergence value of D(q) increased significantly with time. This implies that the spatial diffusion in edge areas was becoming more random and unpredictable, which was hard to control in a short term.

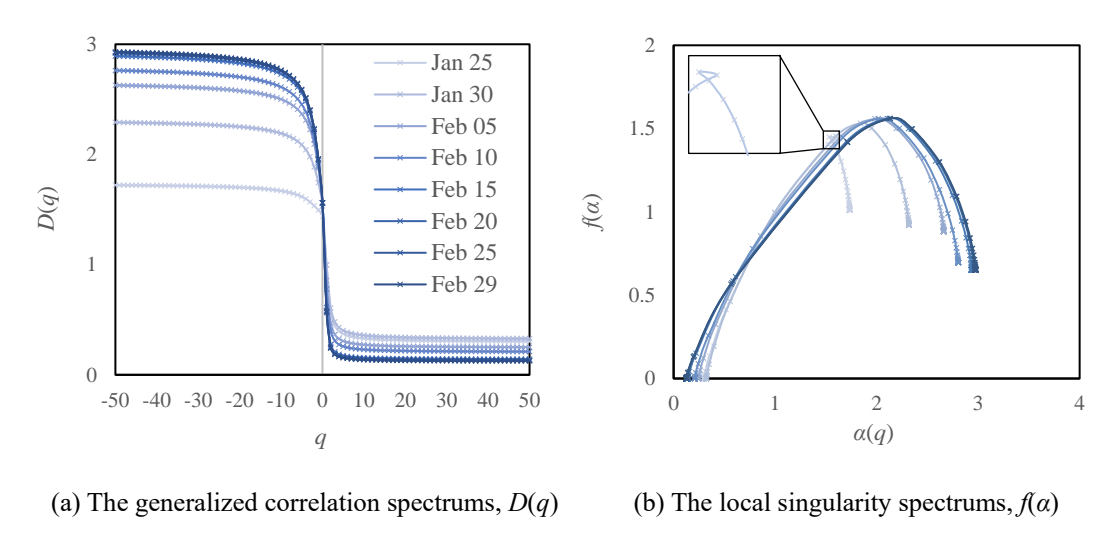


Figure 4. The multifractal spectrums of the spatial diffusion pattern of COVID-19 in Chinese mainland

The local multifractal spectrums reflect the micro mechanism of the spatial epidemic diffusion. The local singularity spectrum $f(\alpha)$ shows two main features: one is the right-leaning unimodal curve, and the other is the local disorder (Figure 4(b)).

Firstly, the $f(\alpha)$ spectrum displays a strongly marked right-leaning unimodal curve, indicating the spatial pattern of COVID-19 takes on global clustering characteristics. There are two basic growth

models of a multifractal system: if the $f(\alpha)$ spectrum is a right-leaning unimodal curve, it represents the growth pattern of spatial concentration; while if the $f(\alpha)$ spectrum takes on a left-leaning unimodal curve, it represents the growth pattern of spatial deconcentration (Chen, 2014a). In Figure 4(b), the $f(\alpha)$ spectrums reveal the spatial concentration pattern of COVID-19, indicating most of the epidemic infections are confined in a few regions, especially around Wuhan as well as cities closely connected with Wuhan. Thus, the timely control measures taken by Chinese government have made positive effects. Otherwise, if the $f(\alpha)$ spectrum is shown as a left-leaning unimodal curve, it implies that the spatial diffusion of COVID-19 would be too rapid to be effectively controlled. Fortunately, that is not the case.

Secondly, the $f(\alpha)$ spectrum shows local disorder, implying the poor-developed fractal structure of COVID-19. In Figure 4(b), there is a twist near the apex of $f(\alpha)$ curve on Jan 25. Besides, the fitting coefficients R^2 of D_1 and D_2 decreased over time (Table 1). These suggest that the quick responses of Chinese government and effective control measures have blocked the spatial diffusion of COVID-19, and further stopped the fractal development of the spatial epidemic diffusion. This is good for the control of COVID-19.

The fractal dimension growth reflects the evolution characteristics of spatial diffusion pattern of COVID-19 (Figure 5). The growth and diffusion are two sides of the same coin. The growth of spatial diffusion with time usually presents as sigmoid curves (Banks, 1988). Let's examine three representative fractal dimensions: D_0 , D_1 and D_2 (Figure 6(a) and Table 2). Firstly, the capacity dimension D_0 roughly reflects the spatial diffusion pattern of COVID-19. The space-filling degree of infected cities in Chinese mainland increased quickly, and then the diffusion rate slowed down. Finally, it formed a constant spatial distribution, no longer spreading to new cities (Figure 5(e)). Secondly, the information dimension D_1 reveals the spatial difference pattern. The spatial uniformity of COVID-19 infections firstly increased, and then the spatial difference increased gradually after Jan 26 (Figure 5(e)). Finally, the spatial distribution of epidemic infections remained stable. The significant decrease on Feb 12 is due to the statistical caliber adjustment of confirmed cases in Wuhan (Figure 6(a)), but it has little effect on the overall trend. Thirdly, the correlation dimension D_2 reveals the spatial correlation of epidemic infections among regions. The spatial correlation degree of the epidemic diffusion reached the strongest very quickly (Figure 5(b)), then became weaker, and finally it was blocked effectively. Thus, the fractal dimension growth of spatial

epidemic diffusion is different from that of cities. Urban growth is a natural process of self-organized evolution. So urban fractal dimension growth is continuous, which can be described by some logistic functions (Chen, 2012; Chen, 2018). Nevertheless, COVID-19 is harmful to human beings, and its growth is affected by the prevention and control measures from human beings in turn. As a result, after a certain level of growth, its fractal dimension would be reduced (Figure 6(a)).

Table 2 The changing trend of three representative generalized correlation dimensions and their reflected geographic information

Parameter	Meaning	Trend	Inference
Capacity	Space-filling	Quasi S-shaped curve.	The spatial distribution range of
dimension D_0	degree	First rise, then tend to	COVID-19 pandemic was expanded
		be stable	first and then converged
Information	Spatial	Firstly, it rose rapidly	The spatial differences of COVID-19
dimension D ₁	uniformity	and then decreased	pandemic were first reduced and then
		gradually	enlarged
Correlation	Spatial	Firstly, it rose rapidly	The spatial correlation of COVID-19
dimension D ₂	dependence	and then decreased	pandemic were first reduced and then
		gradually	enlarged

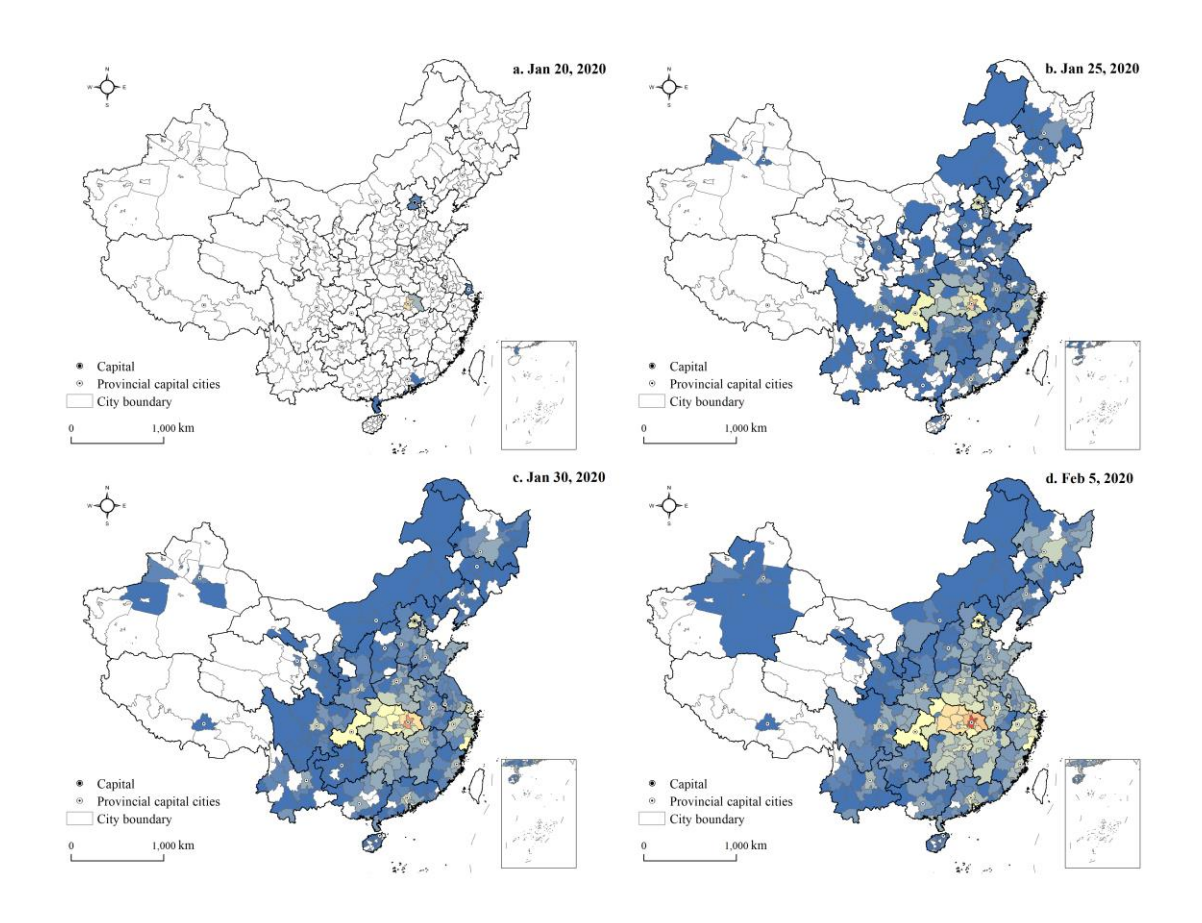
3.3 Stage characteristics of the spatial diffusion of COVID-19

The changing curves of fractal dimensions reflect the stage characteristics of spatial diffusion of COVID-19 (Figure 6(a)). And the stage characteristics reveal the practical effects of prevention and control measures taken by Chinese government. The spatial distribution maps of COVID-19 infections only roughly display the spatial diffusion pattern (Figure 5), which is inconspicuous. In this regard, the changes of fractal dimensions play an irreplaceable role in the spatial analysis of epidemic diffusion. According to the trend of D_0 , D_1 , D_2 and their corresponding spatial meanings, the spatial diffusion pattern of COVID-19 can be divided into 4 stages. The four stages bear analogy with the urbanization curve which can be modeled by logistic function (Chen, 2014b).

① The initial stage. Before Jan 19, the epidemic spread inside Wuhan, showing a single point of

burst. So the fractal dimensions are equal to 0.

② The rapid diffusion stage. From Jan 19 to 26, the space-filling degree (D_0), spatial uniformity (D_1) of the epidemic increased rapidly, and its spatial correlation degree (D_2) reached the highest. These suggest that the infected cities occupied Chinese mainland quickly in large-scale space. In this stage, the long-distance diffusion was the strongest. According to the first law of geography, geographical proximity affects the spatial correlation of regions. So it may be the basis of the spatial epidemic diffusion (Wang *et al.*, 2020). However, in addition to surrounding cities, the epidemic tended to spread to remote cities from Wuhan, such as megacities (i.e., Shenzhen, Beijing, Shanghai), provincial capital cities and some southeastern coastal cities (i.e., Wenzhou, Taizhou) (Figure 5(b)). These cities boast a developed economy and are the main destinations of urban economic connections. It can be inferred that the remote spatial diffusion of COVID-19 may be dominated by economic connections with high liquidity, i.e., tourism and business travel (Shi and Liu, 2020).



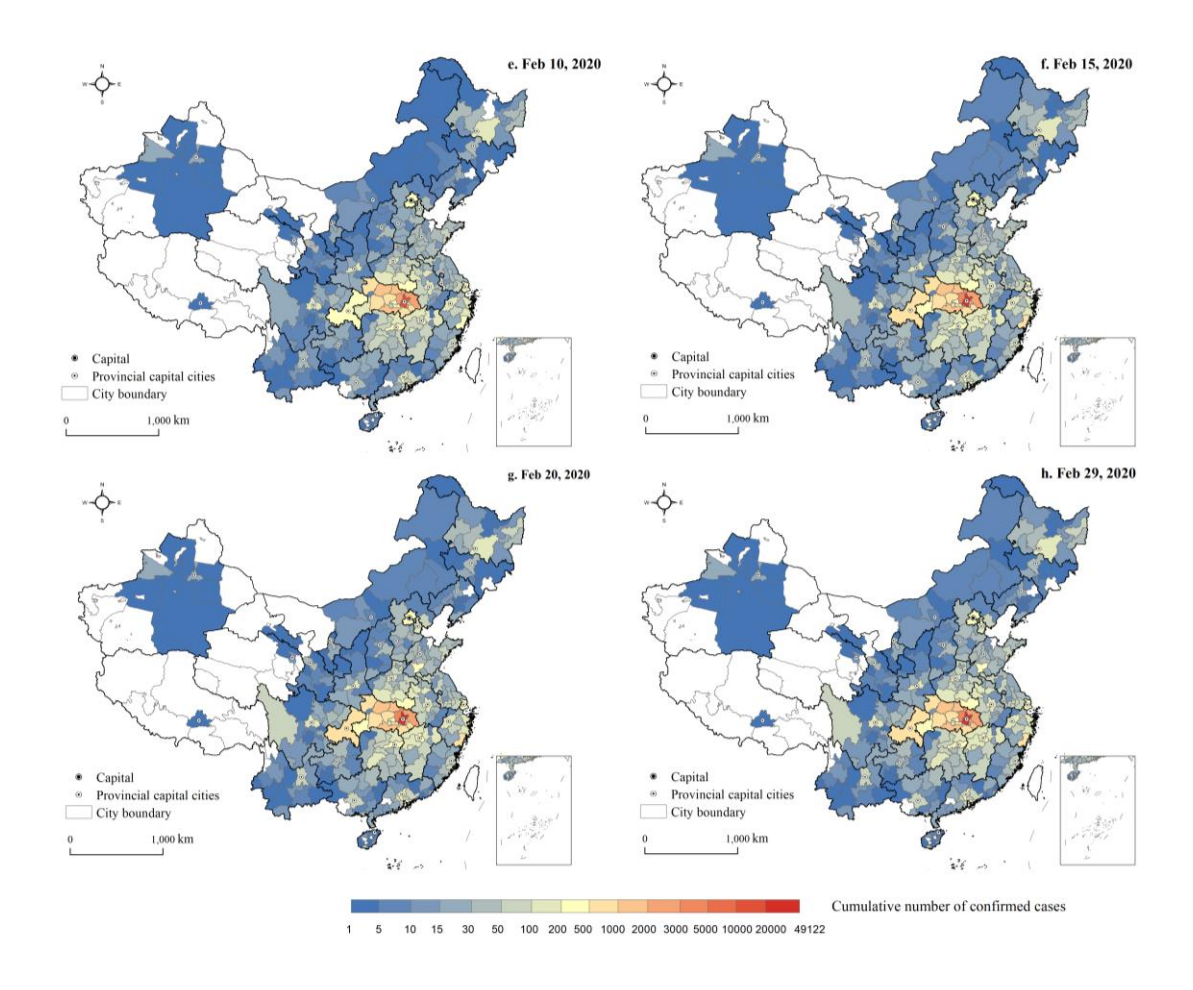


Figure 5. The spatial distribution of COVID-19 infections in Chinese mainland

The deceleration diffusion stage. From Jan 27 to Feb 9, the diffusion rate of infections decreased gradually, and the spatial difference increased. This implies that though more cities were infected, their infections grew slower. While in central regions, their infections grew faster significantly. Besides, the spatial correlation became weaker, implying the epidemic mainly spread to contiguous cities from regional central cities. So it can also be described as the hierarchical diffusion stage, dominated by contagious diffusion. As a whole, the spatial diffusion of COVID-19 infections is seemly bounded by China's population distribution boundary (Hu Huanyong Line) (Figure 2). This line delineates the striking difference in the distribution of China's population: about 96% of the population were settled densely in the eastern half of China, with only 36% of the total area; while a mere 4% of the population were sparsely scattered in the spacious western part (64%) (Hu, 1935). As seen in Figure 2 and Figure 5, the epidemic infections in Chinese mainland are mainly located in the east of 'Hu Huanyong Line', which shares high similarity with the spatial

pattern of population distribution in China.

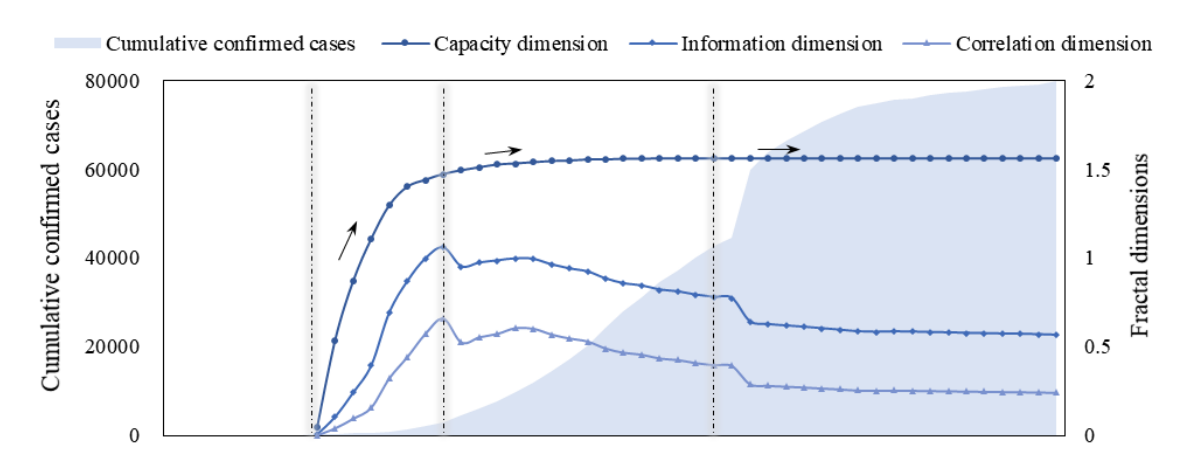
The contraction stage. After Feb 10, the spatial diffusion pattern of COVID-19 reached a relatively stable state. The value of D_0 , D_1 and D_2 gradually converged, reflecting the spatial contraction of epidemic diffusion. About two weeks after the Wuhan lockdown (Jan 23), the spatial diffusion trend of COVID-19 has been successfully controlled in Chinese mainland. Thanks to the implementation of Wuhan lockdown, the remote diffusion was blocked. Besides, the cooperation mechanism on joint prevention and control among regions further blocked the contagious diffusion. This suggests the isolation over regions and reducing inter-regional movement have essentially blocked the spatial diffusion of COVID-19.

Corresponding to the spatial diffusion process of COVID-19, the scale growth of the cumulative number of confirmed cases also presents stage characteristics. Studies have found that the growth of cumulative confirmed cases takes on an S-shaped curve, which can be fitted by logistic model (Martelloni and Martelloni, 2020; Pelinovsky *et al.*, 2020; Consolini and Materassi, 2020; Wang *et al.*, 2020). In this study, two logistic functions are employed to model the scale growth of COVID-19 infections from Jan 11 to Feb 29, due to the statistical caliber adjustment of diagnostic criteria (Figure 6(b)). According to their growth rate and acceleration, the scale growth of COVID-19 can also be divided into 4 stages: the initial stage (before Jan 19), the acceleration stage (Jan 19-Feb 5), the deceleration stage (Feb 6-14) and the late stage (after Feb 14). It can be found that the increase of new confirmed cases reached a peak point on Feb 5. After that, the growth rate slowed down and remained stable in late February. While the spatial diffusion of COVID-19 has reached its peak stage and stable stage earlier. Thus it can be seen that the development of the spatial diffusion process is faster than the scale growth process of COVID-19 (Table 3).

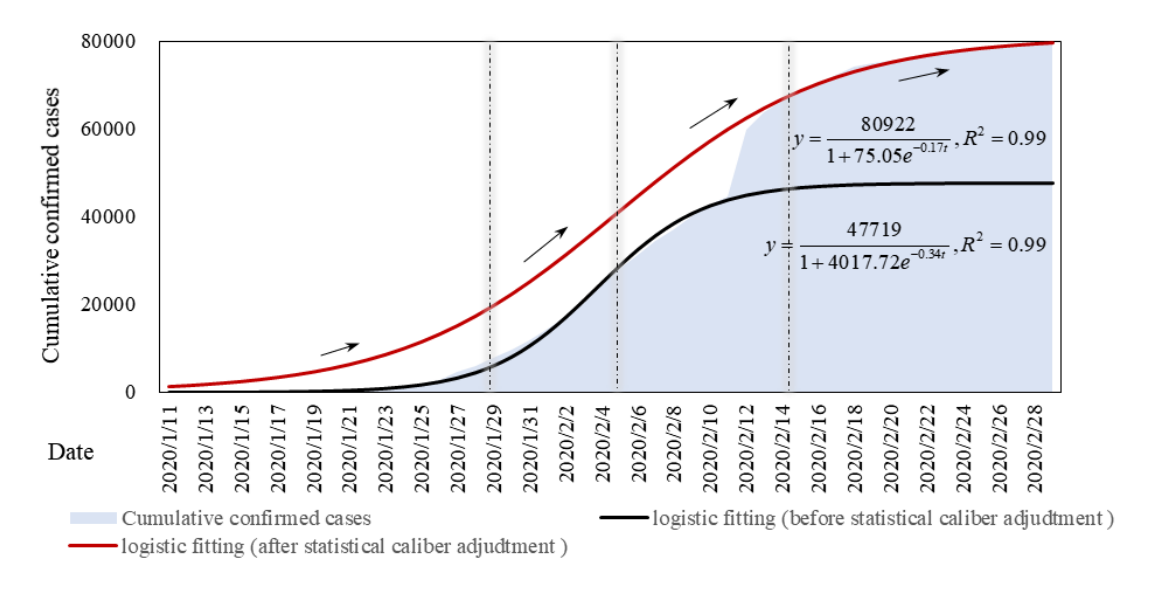
Table 3 Different stages of spatial diffusion process and scale growth process of COVID-19 in Chinese mainland

Stages	es Spatial diffusion		Scale growth	Periods
Stage 1	Initial stage	Before Jan 19	Initial stage	Before Jan 19
Stage 2	Rapid diffusion stage	Jan 19 - 26	Acceleration stage	Jan 19 - Feb 5
Stage 3	Hierarchical diffusion stage	Jan 27 - Feb 9	Deceleration stage	Feb 6 - 14

Stage 4	Contraction stage	After Feb 10	Late stage	After Feb 14
_	_		_	



(a) The spatial diffusion process of COVID-19



(b) The scale growth of COVID-19

Figure 6. The stages of the spatial diffusion and the scale growth of COVID-19

4. Discussion

The above calculations show that the spatial network of COVID-19 infections in Chinese mainland takes on multifractal characteristics. And its distribution pattern and diffusion process can be characterized by multifractal spectrums. The key points of the analyzed results are as follows (Table 4).

Firstly, the spatial pattern of COVID-19 is mainly characterized by global clustering and local diffusion. Though the epidemic infections spread nationwide, few cities were hit severely. In the

global multifractal dimension spectrum, the convergence value of D(q) increased significantly over time when q<0, suggesting the local diffusion of COVID-19 infections (Figure 4(a)). However, the local singularity spectrum $f(\alpha)$ always takes on a right-leaning unimodal curve, implying a global clustering pattern (Figure 4(b)). The epidemic infections in central regions were severe significantly than in marginal regions.

Table 4 Main points of fractal-based spatial analysis for COVID-19 pandemic in Chinese mainland

Item	Feature	Inference
Log-log plot	Straight-line trend	Fractal pattern
Fractal parameters	$D_0 > D_1 > D_2$	Multifractal scaling
Global multifractal spectrum	Inverse S-shaped curve	Multifractal diffusion
Local multifractal spectrum	Right-leaning unimodal	Global clustering, and local
	curve	diffusion
Fractal dimension growth curves	Quasi S-shaped curves	Prevention and control measures
		are effective

Then, the spatial diffusion pattern of COVID-19 in Chinese mainland show stage characteristics, suggesting the positive effects of prevention and control measures taken by the government. According to the fractal dimension growth curves (Figure 6(a)), it can be divided into 4 stages: the initial stage, the rapid diffusion stage, the hierarchical diffusion stage and the contraction stage, from the single point of burst, multi-points spread to the overall outbreak, and finally full containment. And the spatial correlation degree decreased with time. In general, the spatial diffusion of COVID-19 has been contained in a short term. The rapid diffusion stage is the transition period of epidemic diffusion. A series of spatial isolation measures implemented in China has played an important role in the control of COVID-19. As a result, the highly connected population flow was isolated, and the growth rate of infections was effectively reduced. Otherwise, the scale growth of COVID-19 infections in Chinese mainland would not display an S-shaped curve (Figure 6(b)), but rather follows the exponential growth or power-law growth (Brugnago et al., 2020; Omer et al., 2020).

There have been lots of previous studies concentrating on spatial epidemic dynamics. Most of them have described the spatial-temporal pattern of the epidemics by spatial autocorrelation analysis and kernel density estimating (Meng et al., 2005; Wang et al., 2008; Fang et al., 2009; Kang et al., 2020). Nevertheless, a critical problem with these methods is their sensitivity to the spatial scale (Negreiros et al., 2010; Zhang et al., 2019). The novelty of this paper lies in the multifractal scaling model of spatial epidemic diffusion. The spatial diffusion of COVID-19 is a complex process, showing irregular and scale-free features. Given this, fractal analysis is a powerful tool for spatiotemporal modeling of spatial epidemic diffusion from the perspective of scale-free analysis. Multifractal scaling analyses provide two sets of parameters and spectrums, forming a complete understanding of the spatial diffusion pattern of COVID-19 from general to detail. The shortcomings of this study are as below: first, our analysis is based on the COVID-19 dataset from real-time authorized reports, so that the incubation period is not considered. But it has little impact on the overall trend of epidemic evolution. Second, the log-log plots display a poor-developed fractal structure of COVID-19, which may be caused by the data quality. This study takes the prefecturelevel cities as basic spatial units, but the spatial epidemic diffusion is not bounded by the administrative boundary. If there is more accurate location dataset of the confirmed cases, further detailed spatial analysis can be performed in the future.

5. Conclusion

China has effectively contained the COVID-19 pandemic in a short term and has significant performance in this epidemic prevention and control. Modeling the spatial diffusion process and pattern of COVID-19 in Chinese mainland can provide valuable experience for future theoretical and positive studies, and for further improvement of future public health system emergencies. In this work, multifractal scaling model is employed to characterize the spatial diffusion pattern of COVID-19 pandemic, based on the cumulative number of confirmed cases from the authority reports. The main conclusions can be drawn as follows. **First, the spatial pattern of COVID-19 in Chinese mainland bears multifractal characteristics.** Human population pattern may be the geometric support of the multifractal distribution of Covid-19. The inverse S-shaped curves of generalized correlation dimension indicate multifractal property of Covid-19 pandemic. Most of the

population is located in the southeastern part of China. Accordingly, most of the Covid-19 pandemic are located in the southeast China. This implies that the spatial diffusion pattern of COVID-19 has well coincidence relations with the spatial pattern of population in China, both in the geographical distribution and structural hierarchy. Second, the spatial pattern of COVID-19 in Chinese mainland is characterized by global clustering with local diffusion. The unimodal curve of the $f(\alpha)$ curve also suggests the multifractal property of Covid-19 pandemic. The unimodal curve tilts to the right, this suggests that the Covid-19 takes on aggregation pattern in China. That is to say, large-scale infections were confined in central regions, i.e., Wuhan city and its surrounding region. The epidemic situation in other regions was in a controllable state. This suggests the isolation over regions have quickly contained the spatial diffusion of COVID-19. However, the generalized correlation dimension exceeds the Euclidean dimension of embedding space. This implies disordered diffusion of Covid-19 pandemic in some local regions. Third, the spatial diffusion process of COVID-19 in Chinese mainland fell into 4 stages. The fractal dimension growth curves are similar to sigmoid curves. The capacity dimension growth curve reflect the change of space filling process of Covid-19, the information dimension growth curve reflect the change of spatial difference of Covid-19, and the correlation dimension growth curve reflect the change of spatial dependence of Covid-19. The space filling curve increased first and became stable rapidly. The spatial difference and dependence curves increased first and then decreased and finally become stable. By the three curves, the spatial diffusion process of Covid-19 can be divided into four stages: initial stage, rapid diffusion stage, hierarchical diffusion stage, and the contraction stage.

Acknowledgments

This research was sponsored by the National Natural Science Foundation of China (Grant No. 41671167). The supports are gratefully acknowledged.

References

Appleby S (1996). Multifractal characterization of the distribution pattern of the human population.

Geographical Analysis, 28(2): 147-160

Banks RB (1994). Growth and Diffusion Phenomena: Mathematical Frameworks and Applications.

Berlin Heidelberg: Springer-Verlag

- Batty M, Longley PA (1994). Fractal cities: A geometry of form and function. London: Academic press
- Brugnago EL, da Silva RM, Manchein C, Beims MW (2020). How relevant is the decision of containment measures against COVID-19 applied ahead of time? *Chaos, Solitons & Fractals*, 140: 110164
- Caniego FJ, Espejo R, Martín MA, José FS (2005). Multifractal scaling of soil spatial variability. *Ecological Modelling*, 182(3): 291-303
- Chen YG (2012). Fractal dimension evolution and spatial replacement dynamics of urban growth. *Chaos, Solitons & Fractals*, 45(2): 115-124
- Chen YG (2014a). Multifractals of central place systems: Models, dimension spectrums, and empirical analysis. *Physica A: Statistical Mechanics and its Applications*, 402: 266-282
- Chen YG (2014b). An allometric scaling relation based on logistic growth of cities. *Chaos, Solitons & Fractals*, 65: 65-77
- Chen YG (2018). Logistic models of fractal dimension growth of urban morphology. *Fractals*, 26(3): 1850033
- Chen YG (2019). Monofractal, multifractals, and self-affine fractals in urban studies. *Progress in Geography*, 38(1): 38-49 [In Chinese]
- Chen YG, Huang LS (2019). Modeling growth curve of fractal dimension of urban form of Beijing.

 Physica A: Statistical Mechanics and Its Applications, 523: 1038-1056
- Chen YG, Shan WD (1999). Fractal measure of spatial distribution of urban population in a region. *Areal Research and Development*, 18(1): 18-21 [In Chinese]
- Chen YG, Wang JJ (2013). Multifractal characterization of urban form and growth: the case of Beijing.

 Environment and Planning B: Planning & Design, 40(5): 884-904
- Consolini G, Materassi M (2020). A stretched logistic equation for pandemic spreading. *Chaos, Solitons & Fractals*, 140: 110113
- Fang LQ, de Vlas SJ, Feng D, Liang S, Xu YF, Zhou JP, Richardus JH, Cao WC (2009). Geographical spread of SARS in mainland China. *Tropical Medicine & International Health*, 14: 14-20
- Feder J (1988). Fractals (physics of solids and liquids). New York: Plenu
- Frankhauser P (1998). The fractal approach: A new tool for the spatial analysis of urban agglomerations.

 *Population: An English Selection, 10(1): 205–240
- Frankhauser P, Tannier C, Vuidel G, Houot H (2018). An integrated multifractal modelling to urban and

- regional planning. Computers, Environment and Urban Systems, 67: 132-146
- Grassberger P (1983). Generalized Dimensions of Strange Attractors. Physics Letters A, 97(6): 227-230
- Halsey TC, Jensen MH, Kadanoff LP, Procaccia I, Shraiman BI (1986). Fractal Measures and Their Singularities the Characterization of Strange Sets. *Physical Review A*, 33(2): 1141-1151
- Hentschel HGE, Procaccia I (1983). The Infinite Number of Generalized Dimensions of Fractals and Strange Attractors. *Physica D: Nonlinear Phenomena*, 8(3): 435-444
- Hu HY (1935). Essays on China's population distribution. Acta Geographica Sinica, 2(1): 33-74 [In Chinese]
- Huang CL, Wang YM, Li XW, Ren LL, Zhao JP, Hu Y, Zhang L, Fan GH, Xu JY, Gu XY, Cheng ZS, Yu T, Xia JA, Wei Y, Wu WJ, Xie XL, Yin W, Li H, Liu M, Xiao Y, Gao H, Guo L, Xie JG, Wang GF, Jiang RM, Gao ZC, Jin Q, Wang JW, Cao B (2020). Clinical features of patients infected with 2019 novel coronavirus in Wuhan, China. *Lancet*, 395(10223): 497-506
- Kang D, Choi H, Kim JH, Choi J (2020). Spatial epidemic dynamics of the COVID-19 outbreak in China. International Journal of Infectious Diseases, 94: 96-102
- Liu SD, Liu SK (1993). An Introduction to Fractals and Fractal Dimension. Beijing: China Meteorological Press [In Chinese]
- Man W, Nie Q, Li ZM, Li H, Wu XW (2019). Using fractals and multifractals to characterize the spatiotemporal pattern of impervious surfaces in a coastal city: Xiamen, China. *Physica A:* Statistical Mechanics and its Applications, 520: 44-53
- Mandelbrot, BB (1982). The fractal geometry of nature. New York: Freeman
- Martelloni G, Martelloni G (2020). Analysis of the evolution of the Sars-Cov-2 in Italy, the role of the asymptomatics and the success of Logistic model. *Chaos, Solitons & Fractals*, 140: 110150
- Mehta P, McAuley DF, Brown M, Sanchez E, Tattersall RS, Manson JJ, Speciality HA (2020). COVID-19: Consider cytokine storm syndromes and immunosuppression. *Lancet*, 395(10229): 1033-1034
- Meng B, Wang J, Liu J, Wu J, Zhong E (2005). Understanding the spatial diffusion process of severe acute respiratory syndrome in Beijing. *Public Health*, 119(12): 1080-1087
- Murcio R, Masucci AP, Arcaute E, Batty M (2015). Multifractal to monofractal evolution of the London street network. *Physical Review E*, 92(6): 062130
- Negreiros JG, Painho MT, Aguilar FJ, Aguilar MA (2010). A comprehensive framework for exploratory spatial data analysis: Moran location and variance scatterplots. *International Journal of Digital*

- Earth. 3(2): 157-186
- Omer SB, Malani P, del Rio C (2020). The COVID-19 Pandemic in the US A Clinical Update. *JAMA*, 323(18): 1767-1768
- Pavon-Dominguez P, Ariza-Villaverde AB, Rincon-Casado A, de Rave EG, Jimenez-Hornero FJ (2017).

 Fractal and multifractal characterization of the scaling geometry of an urban bus-transport network.

 Computers, Environment and Urban Systems, 64: 229-238
- Pelinovsky E, Kurkin A, Kurkina O, Kokoulina M, Epifanova A (2020). Logistic equation and COVID-19. *Chaos, Solitons & Fractals*, 140: 110241
- Salat H, Murcio R, Yano K, Arcaute E (2018). Uncovering inequality through multifractality of land prices: 1912 and contemporary Kyoto. *Plos One*, 13(4): e0196737
- Semecurbe F, Tannier C, Roux SG (2016). Spatial distribution of human population in France: Exploring the modifiable areal unit problem using multifractal analysis. *Geographical Analysis*, 48(3): 292-313
- Shi QJ, Liu T (2020). Should internal migrants be held accountable for spreading COVID-19? Environment and Planning A: Economy and Space, 52(4): 695-697
- Song ZJ, Yu LJ (2019). Multifractal features of spatial variation in construction land in Beijing (1985-2015). *Palgrave Communications*, 5: 68
- Stanley HE, Meakin P (1988). Multifractal Phenomena in Physics and Chemistry. Nature, 335: 405-409
- Vicsek T (1989). Fractal Growth Phenomena. Singapore: World Scientific Publishing Co
- Wang JF, Christakos G, Han WG, Meng B (2008). Data-driven exploration of 'spatial pattern-time process-driving forces' associations of SARS epidemic in Beijing, China. *Journal of Public Health*, 30(3): 234-244
- Wang JE, Du DL, Wei Y, Yang HR (2020). The development of COVID-19 in China: Spatial diffusion and geographical pattern. *Geographical Research*, 39(7): 1450-1462 [In Chinese]
- Wang PP, Zheng XQ, Li JY, Zhu BR (2020). Prediction of epidemic trends in COVID-19 with logistic model and machine learning technics. *Chaos, Solitons & Fractals*, 139: 110058.
- Wu JT, Leung K, Leung GM (2020). Nowcasting and forecasting the potential domestic and international spread of the 2019-nCoV outbreak originating in Wuhan, China: a modelling study. *Lancet*, 395(10225): 689-697
- YeŞİLkanat CM (2020). Spatio-temporal estimation of the daily cases of COVID-19 in worldwide using

- random forest machine learning algorithm. Chaos, Solitons & Fractals, 140: 110210
- Zhang BE, Xu G, Jiao LM, Liu JF, Dong T, Li ZH, Liu XP, Liu YL (2019). The scale effects of the spatial autocorrelation measurement: aggregation level and spatial resolution. *International Journal of Geographical Information Science*, 33(5): 945-966
- Zhao SL, Chen H (2020). Modeling the epidemic dynamics and control of COVID-19 outbreak in China.

 Quantitative Biology, 8(1): 11-19